Unraveling the Origin of "Turn-On" Effect of Al-MIL-53-NO_2 During H_2S Detection

Zan Zhu, Xiang He, and *Wei-Ning Wang**

Department of Mechanical and Nuclear Engineering, Virginia Commonwealth University, Richmond, Virginia 23219, USA

* Corresponding Author

E-mail: wnwang@vcu.edu

Tel: 1-804-827-4306, 7030 (fax)

S1. BET Surface Area Calculation

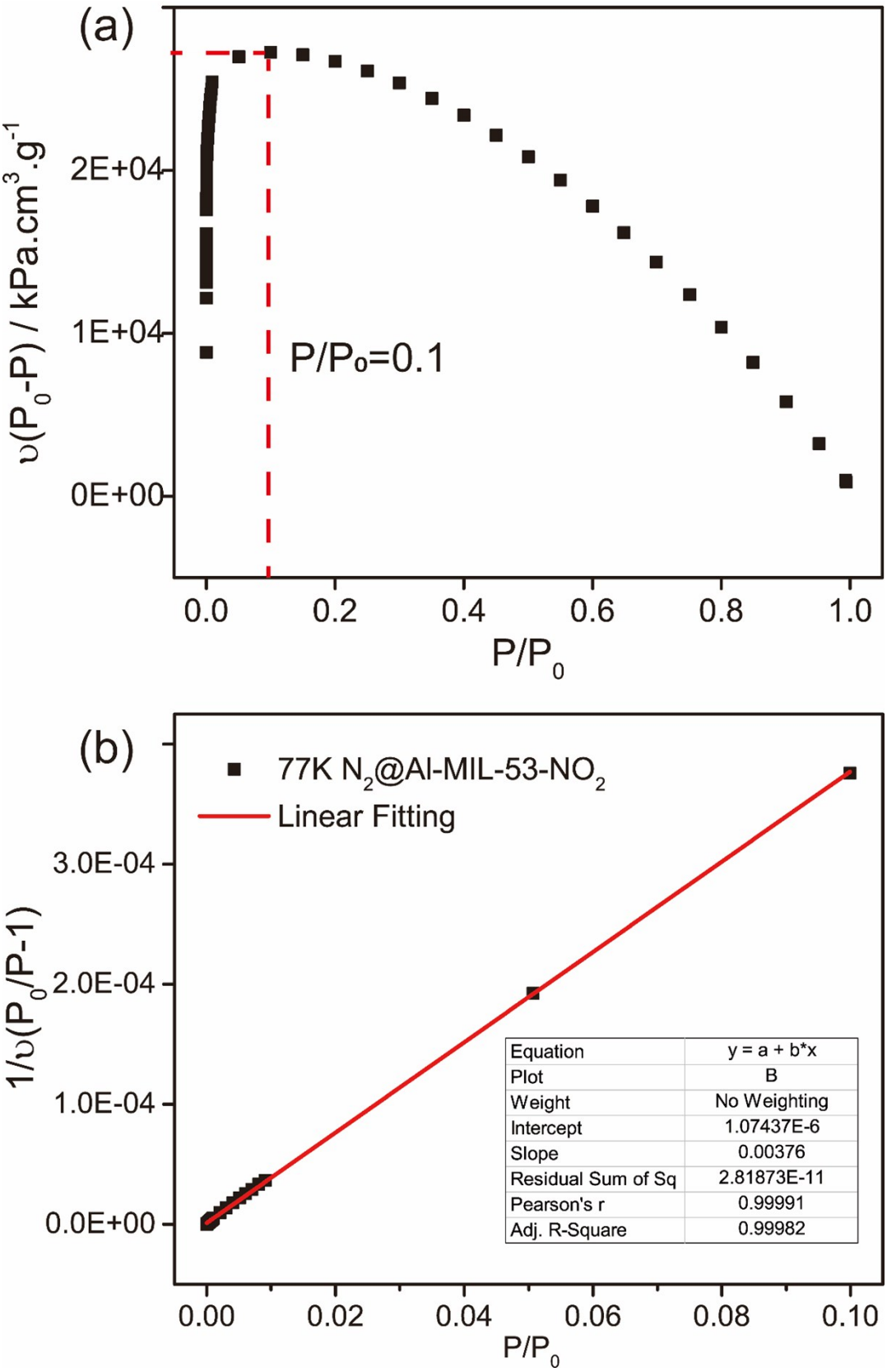

Fig.S1 The consistency plot (a) and BET surface area plot (b) of Al-MIL-53-NO_2.

BET analysis is usually performed during the range of $0.05 < P/P_0 < 0.3$ for typical mesoporous materials. As for the microporous MOFs, BET theory can be also applied if the following criteria are satisfied. [1-4] (a) The pressure range should have values of $v(P_0 - P)$ increasing with P/P_0; (b) The *y*-intercept of the linear region must be positive to give a meaningful value of BET constant *C*; (c) The BET monolayer capacity calculated from the linear fit corresponds to certain relative pressure ($(\frac{P}{P_0})_{v_m}$), which must be located within the linear region chosen for the area calculation. Specifically, the BET surface area is calculated by the equation as follows,

$$S_{BET} = \frac{v_m}{M_v}\sigma_0 N_A$$

where v_m is the monolayer capacity, which could be obtained by the slope ([C-1]/ $v_m C$) and *y*-intercept ($1/v_m C$) ($v_m = \frac{1}{slope + intercept}$); M_v is the molar volume for nitrogen (22414 cm^3); σ_0 is the cross-sectional area of adsorbate (0.162×10^{-18} m^2 for nitrogen); N_A is the Avogadro constant (6.023×10^{23}). Therefore, the BET surface area in this work is calculated as shown below.

$S_{BET} = 1/(1.07437\times10^{-6} + 0.00376)/22414\times6.023\times10^{23}\times0.162\times10^{-18} = 1157$ $m^2\,g^{-1}$;

BET constant $C = 1 + 0.00376/1.07437\times10^{-6} = 3501$;

$$(\frac{P}{P_0})_{v_m} = \frac{1}{\sqrt{C}+1} = 0.0166 \ (0 < 0.0166 < 0.1)$$

S2. Calculation of LOD

The limit of detection (LOD) is calculated according to the following formula:

$$LOD = \frac{3\sigma}{S}$$

where σ is the standard deviation; S is the slope for the suspension and supernatant. [5]

To calculate the LODs of the suspension and supernatant, 0.0015 g Al-MIL-53-NO_2 was treated by various concentrations of H_2S (0.0-0.7 mM). The emission spectra of suspension and supernatant were recorded. By plotting the fluorescence intensity with H_2S concentration (0.0-0.7 mM), the slope for suspension and supernatant were found to be 3.75×10^5 mM^{-1} and 2.07×10^6 mM^{-1}, respectively.

The standard deviation was calculated based on the following equation:

$$\sigma = \sqrt{\frac{\sum(F_i - \bar{F})^2}{N-1}}$$

where F_i is the i^{th} value of fluorescence intensity at 450 nm of suspension/supernatant treated with H_2S from 0.0 mM ($i = 1$) to 0.7 mM ($i = 8$); $\bar{F}$ is the average value of these obtained fluorescence intensities; N is the number of data points (N=8). The calculated standard deviations are shown below.

$\sigma_{suspension} = 86633$

$\sigma_{supernatant} = 481016$

The LODs of suspension and supernatant are thus calculated:

$LOD_{suspension} = 69.3\ \mu M$

$LOD_{supernatant} = 69.7\ \mu M$

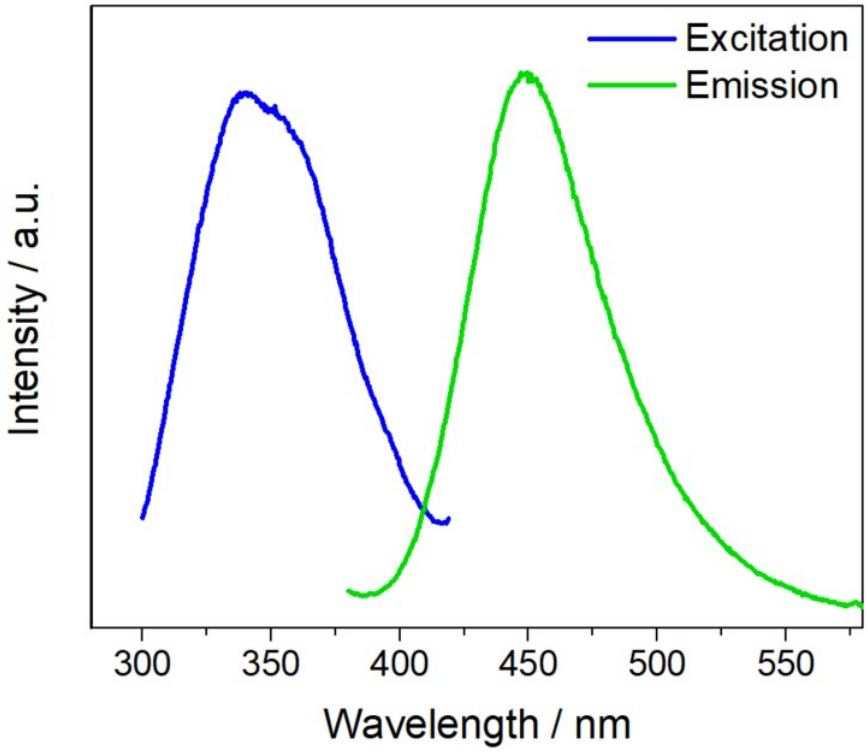

Fig.S2 Excitation (blue line) and emission (green line) spectra of Al-MIL-53-NO_2 upon 1.0 mM H_2S treatment.

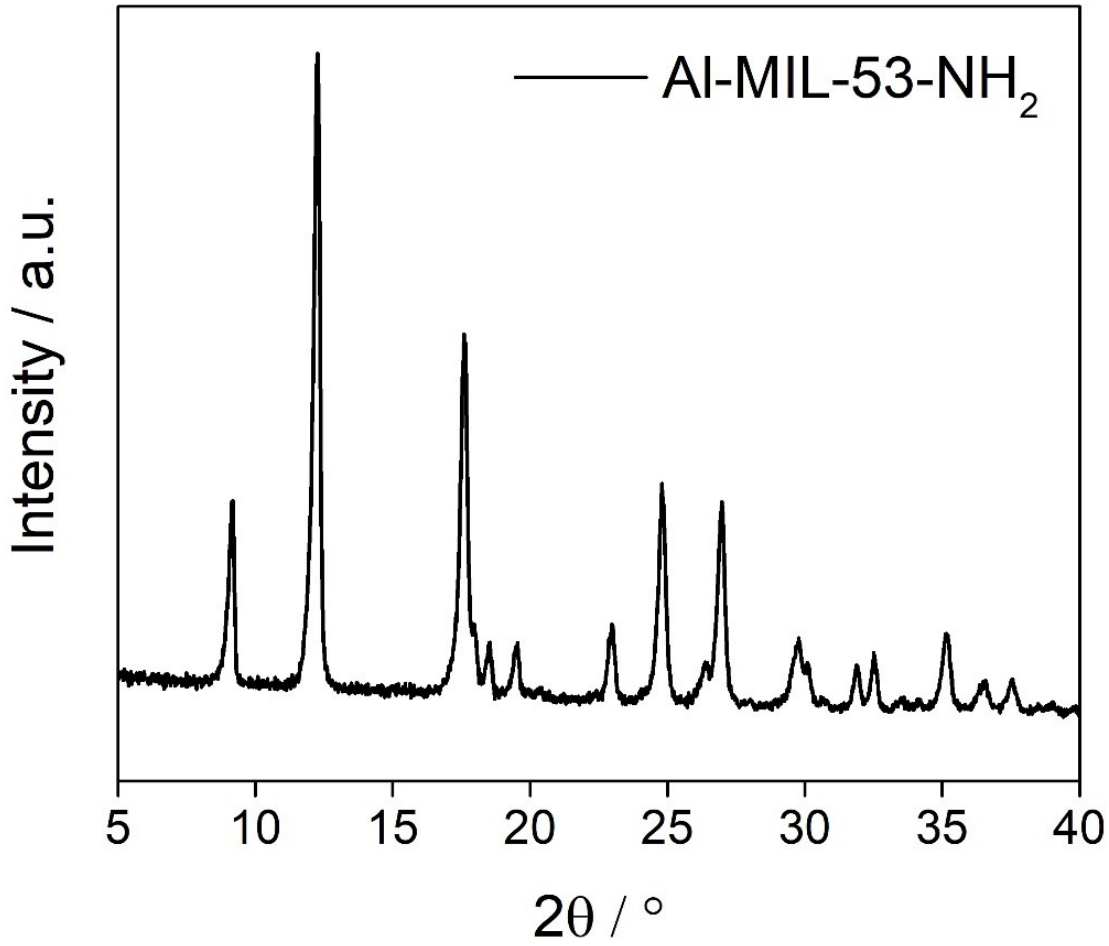

Fig. S3 PXRD pattern of Al-MIL-53-NH_2. The pattern matches well with the previous reference. [6]

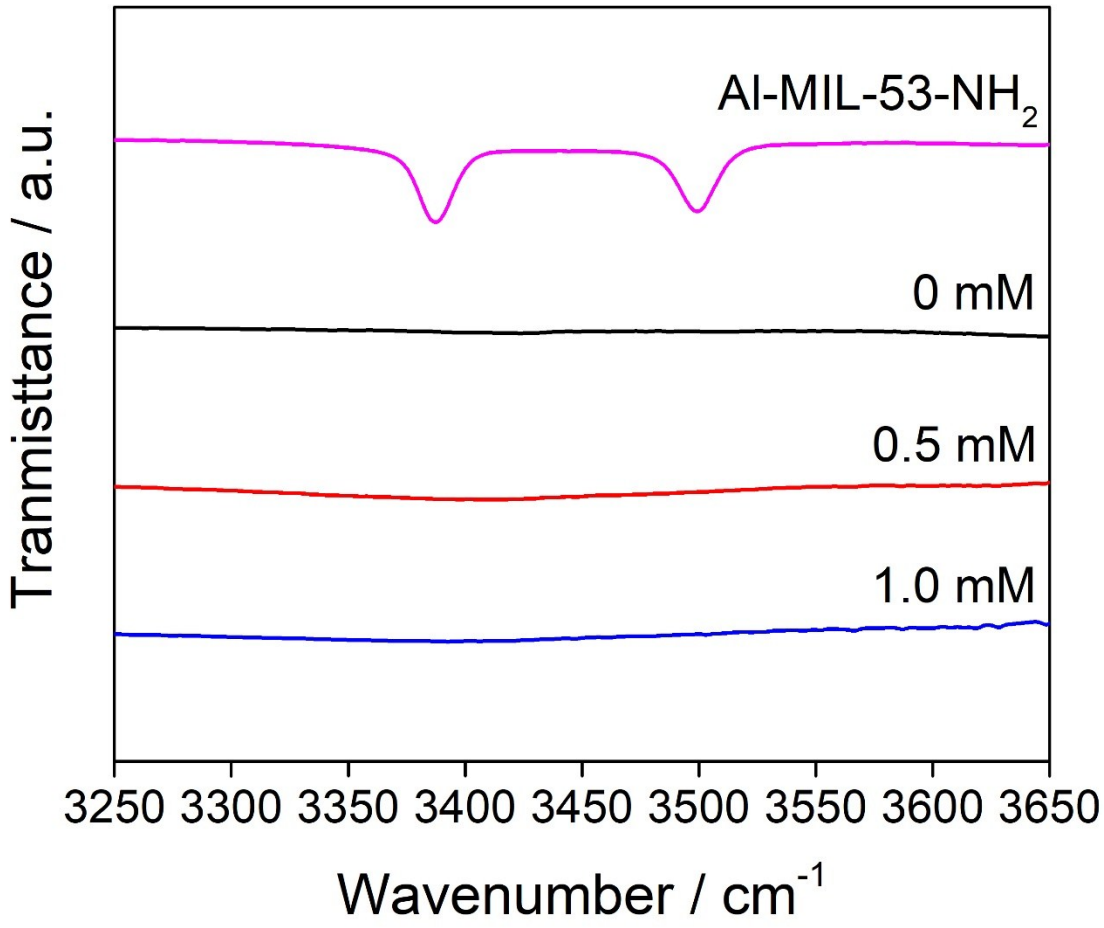

Fig. S4 FT-IR spectra of Al-MIL-53-NH_2 and undissolved Al-MIL-53-NO_2 nanoparticles recollected from 0.0 mM, 0.5 mM, and 1.0 mM NaHS solutions.

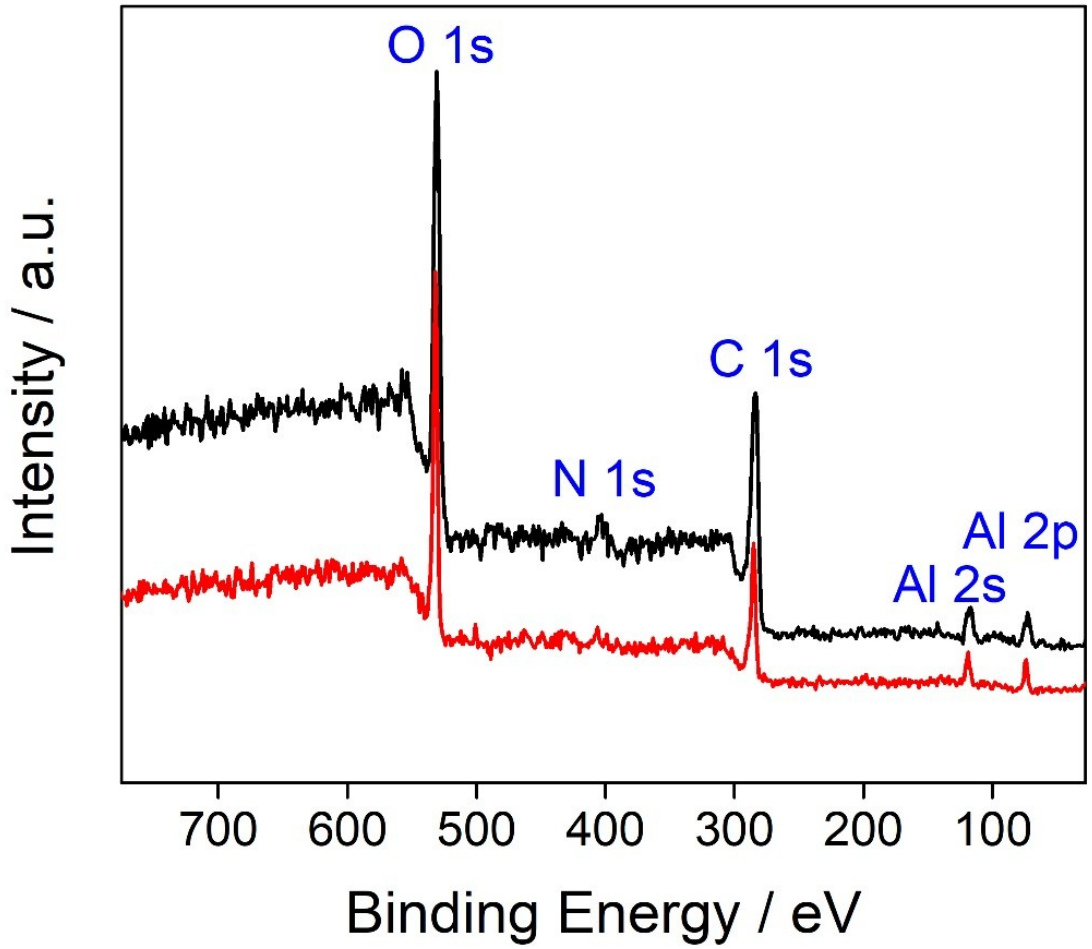

Fig. S5 XPS spectra of Al-MIL-53-NO_2 before (black line) 1.0 mM H_2S treatment and after (red line) 1.0 mM H_2S treatment.

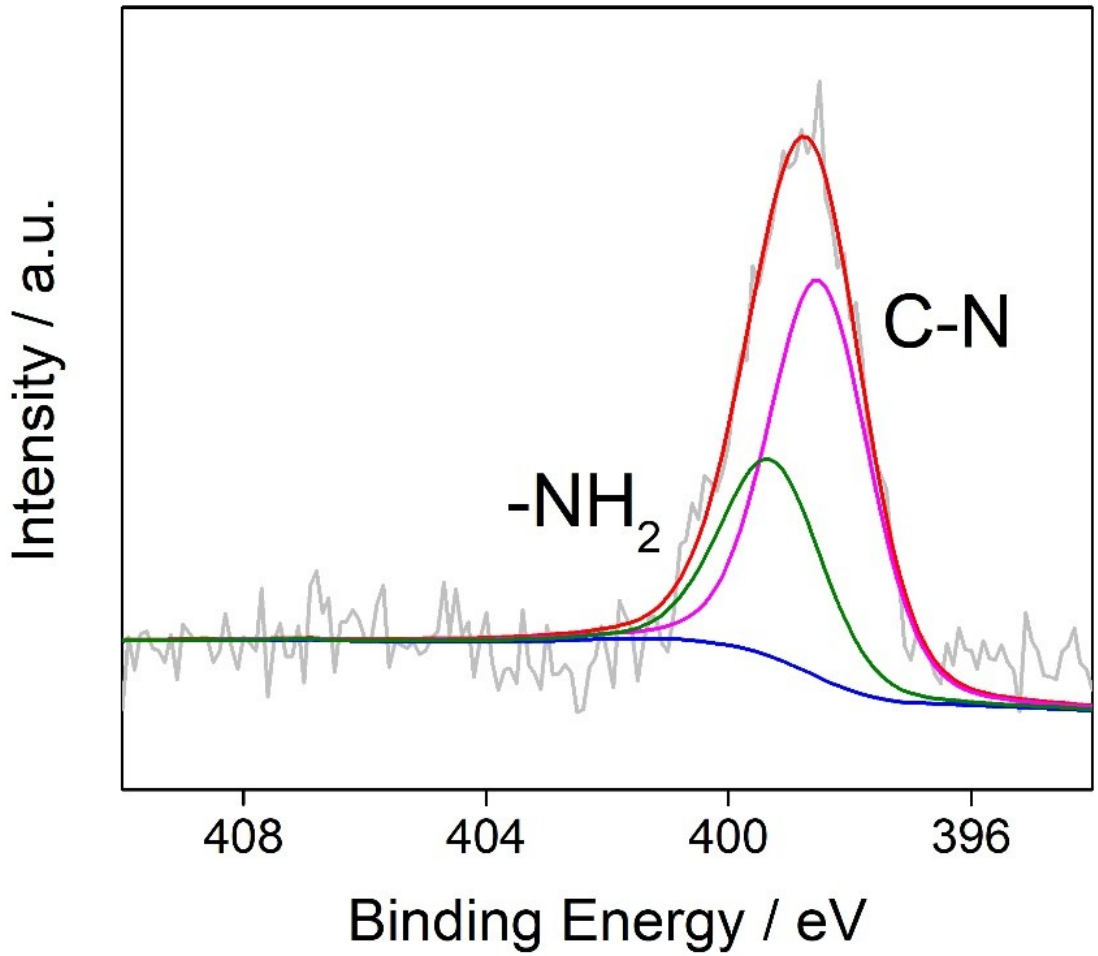

Fig S6. High-resolution XPS spectra of N 1s of as-synthesized Al-MIL-53-NH_2.

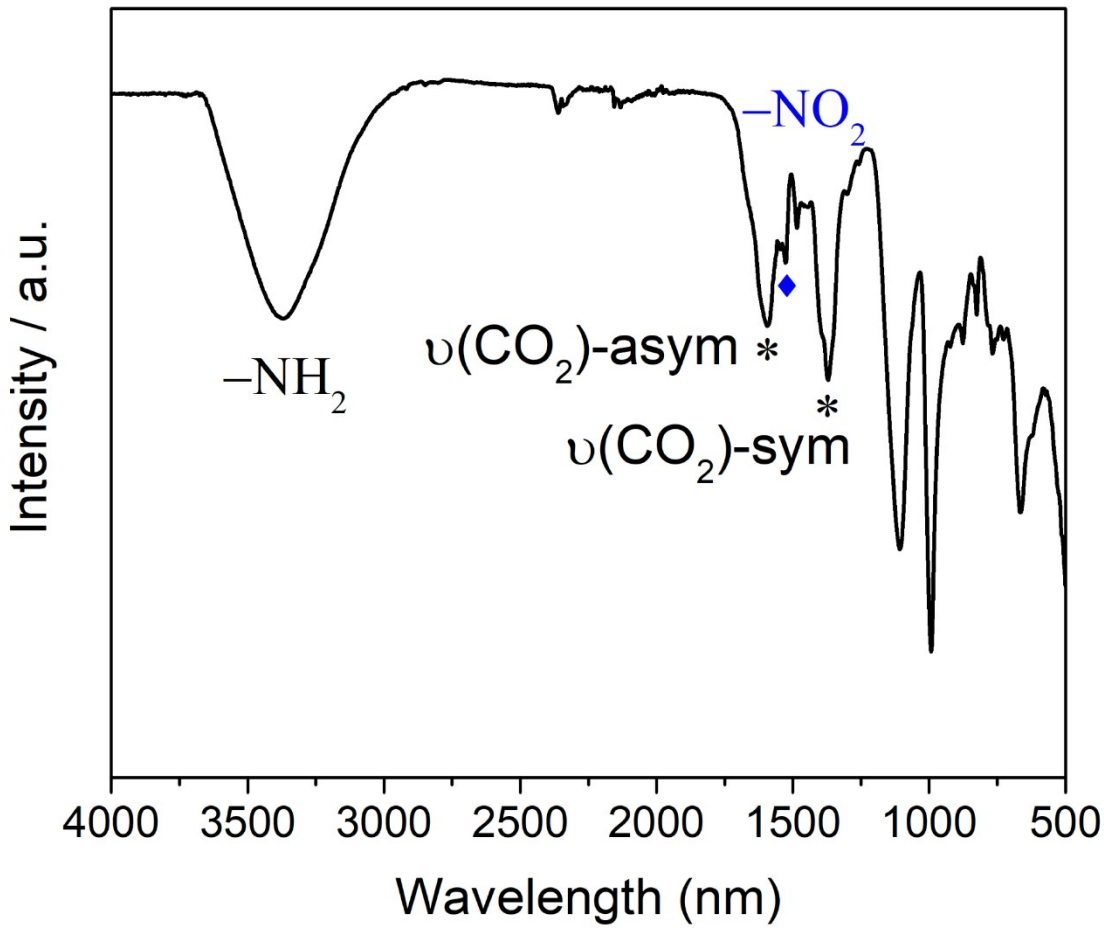

Fig. S7 FT-IR spectrum of extracts evaporated from Al-MIL-53-NO_2 supernatant with 1.0 mM NaHS.

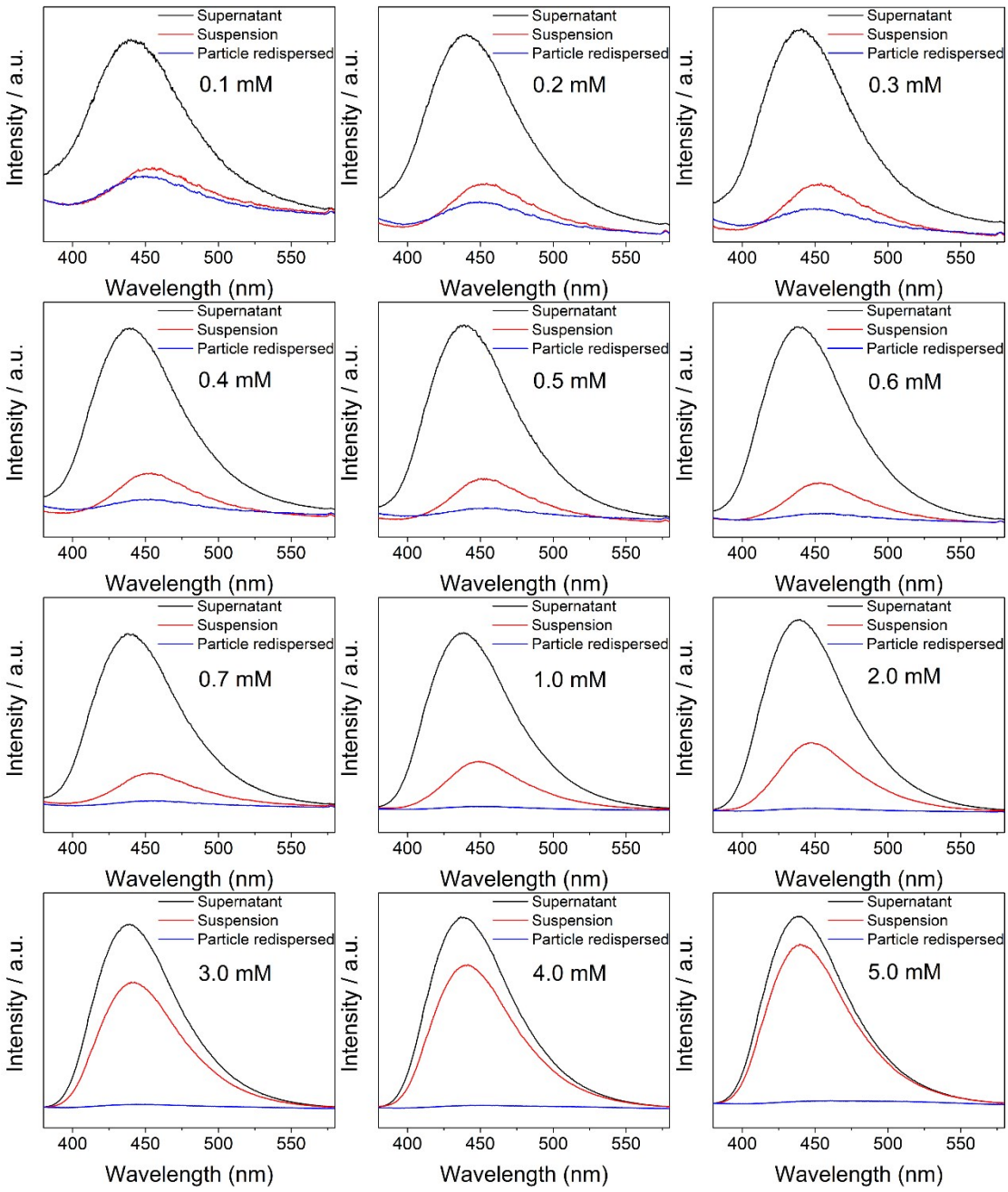

Fig S8. Emission spectra of supernatant, initial suspension, and particles recollected from the suspension of Al-MIL-53-NO_2 treated upon various concentration H_2S.

References:

1. K. S. Walton and R. Q. Snurr, *Journal of the American Chemical Society*, 2007, **129**, 8552-8556.
2. X. He and W.-N. Wang, *Dalton Transactions*, 2019, **48**, 1006-1016.
3. T. Xu, Z. Jiang, M. He, X. Gao and Y. He, *CrystEngComm*, 2019, **21**, 4820-4827.
4. S. Li, J. Wu, X. Gao, M. He, Y. Wang, X. Wang and Y. He, *CrystEngComm*, 2018, **20**, 7178-7183.
5. Y.-Y. Cao, X.-F. Guo and H. Wang, *Sensors and Actuators B: Chemical*, 2017, **243**, 8-13.
6. D. Zhang, Y. Guan, E. J. M. Hensen, T. Xue and Y. Wang, *Catalysis Science & Technology*, 2014, **4**, 795-802.